

Diffusion Kurtosis Imaging Detects Microstructural Changes in the Brain After Acute Carbon Monoxide Intoxication in Rats

Ni LI^a, Gengbiao ZHANG^b, Hongyi ZHENG^b, Weijia LI^b and Wenbin ZHENG^{b,1}

^a *Department of Radiology, The Family Medicine Branch, The First Affiliated Hospital, Shantou University Medical College, Shantou, Guangdong, China*

^b *Department of Radiology, The Second Affiliated Hospital, Shantou University Medical College, Shantou, Guangdong, China*

Abstract. The aim of this study is exploring the value of diffusional kurtosis imaging (DKI) in the diagnosis of acute carbon monoxide poisoning encephalopathy in vivo rats. Forty healthy male Sprague-Dawley rats, were divided into a control group and CO poisoning model group. DKI during 7.0 T MR were performed in the globus pallidus, hippocampus and parietal cortex in the rats. During acute CO poisoning, compared with controls, Mean kurtosis values (MK) and Mean diffusivity (MD) values were significantly decreased both in the hippocampus and parietal cortex, however, in the globus pallidus were significantly increased. The pathological findings showed emerged granular cytoplasmic changes, thickening of chromatin of the neurons, and local lymphocytic infiltration. However, the condition in the hippocampus and parietal cortex was significantly milder than in the globus pallidus region in the first day or 3 days later. Both Immunohistochemical analysis of the heme oxygenase-1 of rats and MK values increased only in globus pallidus with a statistical difference between the CO poisoning group and the normal group both in the day 1 and day 3. DKI can possess sufficient sensitivity for tracking pathophysiological changes associated with carbon monoxide intoxication. The higher MK values in acute stage of carbon monoxide intoxication might indicate poor prognosis in the evolution of the condition.

Keywords. Magnetic resonance imaging, diffusion kurtosis imaging, carbon monoxide poisoning encephalopathy

1. Introduction

Acute Carbon Monoxide (CO) poisoning is still the leading cause of acute poisoning-related death in China. The central nervous system is the part of the body most sensitive to hypoxia. In this way, acute Carbon Monoxide (CO) poisoning often shows varying alterations with cognitive dysfunctions, such as learning and memory deficits and degrees of neurological sequelae [1, 2]. The severity of the symptoms of patients with brain damage cannot be compared directly, so, clinically, there are many obstacles

¹ Corresponding Author, Wenbin ZHENG, Department of Radiology, The Second Affiliated Hospital, Shantou University Medical College, Shantou, Guangdong, China; Email: hwenb@126.com.

to the evaluation of early brain damage in these patients.

Encephalopathy caused by acute CO poisoning showed lesions in the cerebral cortex and basal ganglia (mainly involving the globus pallidus) on early magnetic resonance imaging (MRI). Although conventional MRI can show the morphological changes in the brain after CO poisoning [3, 4], it lacks a clear quantitative parameter that could be used to measure the extent of the damages.

Studies assessing prognosis of CO poisoning using different forms of MR diffusion tensor imaging (DTI) technology showed that, at the subacute or chronic phase of acute carbon-monoxide-poisoning-related encephalopathy, the direction of water molecule diffusion is reduced due to demyelination, so Fractional anisotropy (FA) values may decrease [5, 6]. These decreases in FA values in acute carbon monoxide poisoning are associated with deterioration of the symptoms of encephalopathy, and the increase in FA values may associated with improvement of the symptoms. DTI has tremendous value in evaluating brain damage after CO poisoning [7, 8], but it mainly involves the assessment of damage in the deep white matter. However, DTI measurements are based on the assumption of a Gaussian displacement probability distribution of water molecules due to water self-diffusion [9], making DTI a limited indicator of complexity.

This limitation can be partially overcome with diffusional kurtosis imaging (DKI), a newly emerging MRI modality based on the non-Gaussian diffusion of water in biological systems. With DKI, not only the conventional DTI parameters are derivable, but also complexity and heterogeneity of the microenvironments could also be distinguished, thereby indicating the potential of being a more sensitive biomarker than DTI to brain pathophysiological changes. A scalar index derived from DKI called the mean kurtosis (MK) has been shown to be sensitive to structural changes in both anisotropic tissue, such as white matter (WM), and isotropic tissue such as Gray Matter (GM) and therefore may provide information on tissue microarchitecture complementary to that given by fractional anisotropy and mean diffusivity [10]. Current preliminary studies of DKI in human and rat brain tissue infarction, multiple sclerosis, attention deficit hyperactivity disorder, Parkinson's disease, Alzheimer's disease, gliomas, and other central nervous system diseases have achieved significantly favorable results. DKI scanning can simultaneously measure multiple parameters, such as fractional anisotropy (FA), mean diffusivity (MD), mean kurtosis (MK), which plays a very important role in the assessment of disease progression and prognosis [11, 12].

Therefore, we hypothesized that DKI could improve the early description and histological evidence of encephalopathy in a rat model of CO poisoning.

2. Materials and Methods

2.1. Ethics Statement

This study was carried out in strict accordance with the recommendations in the Guide for the Care and Use of Laboratory Animals of the National Institutes of Health. The protocol was approved by the Committee on the Ethics of Animal Experiments of the Shantou University Medical College of China. All surgery was performed under isoflurane anesthesia, and all efforts were made to minimize suffering.

2.2. Study Animals

Forty healthy male Sprague-Dawley rats, weighing 195-220 g (mean 205.23 ± 14.189 g) were kept at room temperature for one week in an animal room to allow them to adapt to the experimental conditions. Feeding environment: light-dark cycle at every 12h, temperature at 22 degrees Celsius, relative humidity at 55%, food and water were provided ad libitum and rats were housed in groups.

The rats were divided into a control group (NC group, n = 20, intraperitoneal injection of air for control) and CO poisoning model group (n = 20). Pure CO gas (99.95%) was provided by the Kede Gas Co., Foshan, China.

2.3. Carbon Monoxide Poisoning Rat Model and Observation

After weighting, Sprague-Dawley rats were intraperitoneally injected with 150 ml/1000 gCO [13]. After 1 h of CO exposure, the animals presented with less activity, limp limbs, convulsions, cherry red limb skin, and some rats showed brief coma. The characteristic limb limpness and cherry red skin at the extremities were considered indicative of successful modeling. Two of the 20 rats died, and the remaining 18 rats were included in the CO group. The NC group was injected intraperitoneally with the same amount of air. No abnormalities were observed in the NC group.

2.4. 7.0T MRI Scanning and Post-Processing

All rats were scanned on an Agilent 7T/160 mm animal MR scanner (Agilent VnmrJ 3 Imaging, USA) which used a single-channel body coil as transmitter and receiver coils. The 20 rats of control group and 18 rats exposed to CO in the successful modeling group were imaged on day1, and 20 rats in NC group and 9 rats in CO group were immediately sacrificed for histology after all images were acquired, and the remaining 9 rats in CO group were fed routinely for another 3 days, and were also sacrificed for histology after all images were acquired on day 3.

During the process of scanning, all the animals were anesthetized with 4% isoflurane mixed with 1 L/min oxygen and maintained with 2% isoflurane. Respiratory changes were observed in real time using breath monitoring to maintain at 50-60 times for every minute. Each animal's arterial blood had been drawn from the left atrium and blood HbCO levels were measured to determine level of CO within 30 minutes using ultraviolet-visible light detector (Gem Premier 3000, Dechang Tech. Co. Ltd, Guangzhou).

Before scanning, 4 certain collections of parameters, which are quick scout, volume scout, brain shim and shimming check, were run to ensure the MRI scanner is properly adjusted for the best performance. The scan sequence included T2WI sequence and DKI sequence.

T2-weighted imaging was obtained using a 2D fast spin echo (FSE) sequence: (Repetition time, TR)/Effective (Echo time, TE)=1500ms/40ms, NEX(number of excitation)=2, field of view (FOV)=30mm×30mm, and the data matrix (Frequency Coding × Phase encoding) of 256×256 using 6 slices at 2mm thickness without gap). For FSE echo-spacing is 6.616ms and the echo train length is eight.

Diffusion kurtosis imaging was obtained with EPIP sequence, which is the Agilent improved version of Echo Planar Imaging, together with a data matrix (RO×PE) of 128×128 and a TR/TE of 2000ms/36ms at 2 mm thickness without gap, NEX=2 and 4

shots. For EPIP echo-spacing is 0.648 ms and the echo train length is 32. Two b-values (1000 s/mm^2 and 2000 s/mm^2) were applied to 30 directions following acquisition of the image at $b = 0 \text{ s/mm}^2$. The average duration time for the DKI scan was approximately 33min7s.

Data measurement techniques: We used the DKE software (version 2.5.0e), which downloaded by the Internet (<http://academicdepartments.musc.edu/cbi/dki/dke.html>), then modified the Agilent data format as DICOM and processed in the MATLAB (The Mathworks, Natick, MA, USA). We used MATLAB to process the image between T2WI and DKI. T2 image sequences were referred for anatomical positioning. The images were registered with the co-registration option available in the DKE program and motion corrected were using SPM. In the process of data acquisition, we reduced the impact of eddy currents by optimizing the scanning parameters. Thus, we used a sequence which based on the EPIP with a smaller TE time and had a less affection on the eddy currents. The globus pallidus, hippocampus, and parietal cortex were treated as three different groups and a total of six ROIs (every region of interest was about 5mm^2), e.g., left and right globus pallidus, left and right hippocampus, left and right parietal cortex (Figure 1). Regions of interest (ROIs) were manually defined in several coronal slices by referencing to the standard rat brain atlas [14]. Anatomical landmarks were identified from both FA and MK maps in each animal [15].

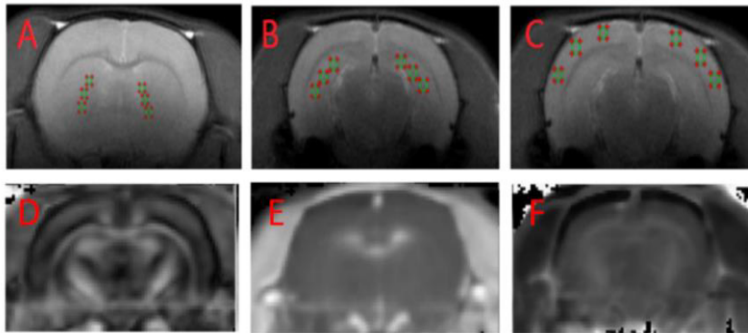


Figure 1. A-C The anatomical location and ROI placement of the globus pallidus (A), hippocampus (B) and parietal cortex (C) were in accordance with the T2 sequence. D-F The diffusion image of FA (D), MD (E) and MK (F) value.

2.5. Histology

After all images were obtained, all the rats were immediately killed for histology. They were anesthetized with 4% isoflurane mixed with 1 L/min oxygen and maintained with 2% isoflurane during the whole process. Brains were removed and fixed with 4% paraformaldehyde for 48h. After fixation, brains were embedded in paraffin, and contiguous $4\mu\text{m}$ sections at the level of the globus pallidus, hippocampus and parietal cortex were cut on a microtome (Rm 2016, LEICA, Germany).

Some sections were then stained with hematoxylin and eosin (HE). The other sections were deparaffinized in xylene, rehydrated in a descending series of ethanol solutions, and then treated with 0.3% hydrogen peroxide methanol solution for 10 min to quench endogenous peroxidase activity. To block non-specific staining, we incubated sections with the boiling Tris-EDTA buffer (pH=9.0, 95-100°C) for 20 min. After

cooling at room temperature for 10 mins, the sections were decolorized in PBS (pH=7.4) for 10 mins and added 1%BSA for 20 min after drying. Next, primary antibodies for the Heme oxygenase -1 were added, and the slides were incubated at 37°C for 1h. After washing with PBS, corresponding secondary antibodies were added for incubation at room temperature for 30 min before reaction with diaminobenzidine and counterstaining with hematoxylin. All the sections were then dehydrated and mounted.

Images were captured using a Leica IM50 microscope at $\times 200$, and three different fields for each ROI were selected in each sample. The value of integrated optical density of ROIs in images were then counted with the application of Image-pro plus 6.0 Software (Media Cybernetics, Inc., Rockville, MD, USA).

2.6. Statistical Methods

Data analysis was conducted using SPSS 20.0 (SPSS Inc., Chicago, IL, USA) software. Each of the measured parameters (MD, FA and MK) was expressed as mean \pm standard deviation. The average MK, FA, and MD values were calculated bilaterally on the left and Right sides in the ROIs and done normal distribution test. Using a single sample K-S test of nonparametric test, a level of $P > 0.05$ was considered that the data are approximately normally distributed. The data accorded with normal distribution were compared by Pair t-test, otherwise, by Mann-Whitney test. The average values of FA, MD and MK of the ROIs, which are normally distributed, between the CO exposed group and the normal control group were compared with the independent sample t test. A level of $P < 0.05$ was considered statistically significant.

3. Experimental results

3.1. HbCO Level

All the animals were taken 150mL/kg does of CO peritoneum injection, and their blood HbCO levels ranged from 58.2% to 75%, with an average of 64.53%.

3.2. Comparison of FA, MD and MK Values

The comparison of the mean values of FA, MD and MK (Figures 2D-2F) between the left and right sides showed no statistically significant differences ($P > 0.05$). The left and right ROIs were averaged for the group comparison. For the CO poisoning model group, MK values were 0.70 ± 0.02 , 0.62 ± 0.01 , 0.80 ± 0.13 on day1 and 0.63 ± 0.15 , 0.64 ± 0.12 , 0.69 ± 0.14 on day3 in the three ROIs. Compared to the normal control group, MK values were found to be lower in the hippocampus and parietal cortex, and MK values in the globus pallidus were statistically significantly higher in the CO-exposed rats. MD values were 0.76 ± 0.05 , 0.83 ± 0.17 , 0.79 ± 0.13 on day1 and 0.84 ± 0.09 , 0.85 ± 0.15 , 0.74 ± 0.05 on day3 in the three ROIs. MD values were found to be lower in the hippocampus and parietal cortex of rats in the CO exposure group than in normal control rats, and higher in the globus pallidus. FA values were 0.18 ± 0.08 , 0.20 ± 0.08 , 0.30 ± 0.09 on day1 and 0.24 ± 0.10 , 0.25 ± 0.09 , 0.42 ± 0.11 on day3 in the three ROIs. FA values were found to be statistically significantly lower in the hippocampus in rats that

had been exposed to CO than in the normal control group. However, FA values did not show significant differences in the parietal lobe and globus pallidus between the CO exposed and normal control rats. Mean values of FA, MD, and MK and statistical comparisons of the CO exposed and control groups are detailed in Table 1.

3.3. Correlation between the MK Values and the Carboxyhemoglobin Levels

The MK values of the right and left globus pallidus, hippocampus and parietal cortex showed no significant correlations with COHb levels (all $p > 0.05$) (Table 2).

3.4. HE Staining of the Rat Brain

Eighteen rats exposed to CO in the successful modeling group were randomly prepared for tissue dissection and HE staining after brain MRI scan on Day 1 and Day 3. Under light microscope (HE $\times 400$), the brain tissue from the normal control rats of parietal cortex showed normal morphology. Eighteen rats exposed to CO in the successful modeling group were randomly prepared for tissue dissection and HE staining after brain MRI scan on Day 1 and Day 3. Under light microscope (HE $\times 400$), the brain tissue from the normal control rats of parietal cortex showed normal morphology and the neurons arranged orderly on a pale pink background (Figure 2a). On Day 1 group, light microscopy showed increased space between the neurons around the hippocampus and parietal cortex. Three days later, rats in the CO exposure group showed the brain tissue in parietal cortex or in the hippocampus (HE $\times 400$) (Figure 2b), only with fewer nervous cells with light staining of the nuclei, suggesting with cerebral edema.

Table 1. Comparison of DKI values of the hippocampus, globus pallidus and parietal cortex in the rats exposed group and the normal control group (Mean \pm SD).

DKI values	Control (n=20)	DAY1 (n=18)	DAY3 (n=9)
hippocampus			
MK	0.82 \pm 0.06	0.70 \pm 0.02**	0.63 \pm 0.15**
FA	0.15 \pm 0.03	0.18 \pm 0.08	0.24 \pm 0.10**
MD [10-3mm ² /s]	1.18 \pm 0.06	0.76 \pm 0.05**	0.84 \pm 0.09** §
parietal cortex			
MK	0.95 \pm 0.03	0.62 \pm 0.01**	0.64 \pm 0.12**
FA	0.30 \pm 0.02	0.28 \pm 0.08	0.29 \pm 0.09
MD [10-3mm ² /s]	1.19 \pm 0.07	0.83 \pm 0.17**	0.85 \pm 0.15**
globus pallidus			
MK	0.81 \pm 0.05	0.96 \pm 0.13**	0.69 \pm 0.14** §
FA	0.20 \pm 0.05	0.30 \pm 0.09	0.42 \pm 0.11**§
MD [10-3mm ² /s]	0.98 \pm 0.03	0.79 \pm 0.13*	0.75 \pm 0.05*

* $P < 0.05$ was considered to indicate a statistically significant difference; ** $P < 0.01$ was considered to indicate a clear statistically significant difference; * Statistical significance was based on comparison with controls; § Statistical significance was based on comparison with DAY1.

Table 2. Correlations between the MK values in the bilateral globus pallidus, hippocampus, and parietal cortex with the carboxyhemoglobin levels in the acute CO rats.

	Correlation coefficient	P
Right globus pallidus	0.445	0.0512
Left globus pallidus	0.546	0.0622
Right hippocampus	0.373	0.4831
Left hippocampus	0.366	0.3865
Right parietal cortex	0.271	0.4321
Left parietal cortex	0.287	0.5772

The cells of globus pallidus region, the normal control rats showed normal morphology with very large neurons and very large dendritic arborizations. (HE×400) (Figure 3a), the CO exposure group in first day showed granular cytoplasm changed and dark stain in the cells of globus pallidus region, nuclear pyknosis of neurons, and glial cells mildly increasing. (HE×400) (Figure 3b). Three days later after CO exposure showed swelling of neurons, vacuolar degeneration, blurry outline of the cells, fuzzy nucleolus, nuclear pyknosis and more glial cells in globus pallidus (HE×400) (Figure 3c).

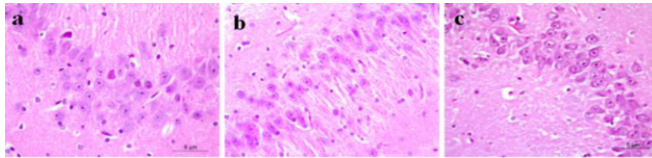


Figure 2. The brain tissue of hippocampus:(a) Under light microscope, the normal control rats showed normal morphology and the neurons arranged orderly. (HE ×400). (b) The CO exposure group in first day, light microscopy showed increased space between the neurons around the hippocampus. (HE×400). (c) Three days after CO exposure, showed fewer nervous cells with dark staining of the nuclei. (HE×400).

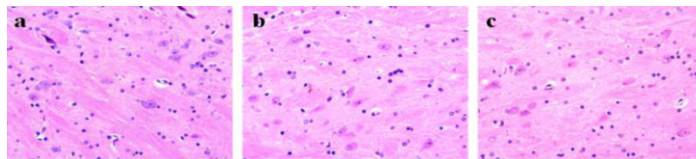


Figure 3. The cells of globus pallidus region: (a) The normal control rats showed normal morphology with very large neurons and very large dendritic arborizations. (HE×400). (b) The CO exposure group in first day showed granular cytoplasm changed and dark stain in the cells of globus pallidus region, nuclear pyknosis of neurons, and glial cells mildly increasing. (HE×400). (c) Three days later after CO exposure showed swelling of neurons, vacuolar degeneration, blurry outline of the cells, fuzzy nucleolus, nuclear pyknosis and more glial cells in globus pallidus. (HE×400).

3.5 Immunohistochemical analysis of the heme oxygenase-1(HO-1)

The result of immunohistochemical experiments of the heme oxygenase-1 of rats showed the IOD of the heme oxygenase-1 expression in the globus pallidus were increased in the CO poisoning group (Figure 4). There was a statistical difference between the CO poisoning group and the normal group both in the day 1 and day 3, while there is no statistically significant difference of the IOD of the heme oxygenase-1 expression in the the hippocampus and parietal cortex between the CO poisoning group and the normal group both in the day 1 or day 3 (Table 3).

Table 3. Comparison of integrated optical density (IOD) value of the hippocampus, globus pallidus and parietal cortex in the rats CO exposed group and the normal control group. (Mean±SD).

	Control (n=4)	DAY1 (n=4)	DAY3 (n=4)
Globus Pallidus	10550.10±4362.32	17149.15±4362.32*	19429.16±4220.72*
Parietal Cortex	8483.02±2134.92	6704.14±2629.44	8335.94±590.45
Hippocampus	12003.12±5785.52	8347.88±7642.77	12837.27±5887.87

*P<0.05 was considered to indicate a statistically significant difference; **P<0.01 was considered to indicate a clear statistically significant difference; * Statistical significance was based on comparison with controls; § Statistical significance was based on comparison with DAY1.

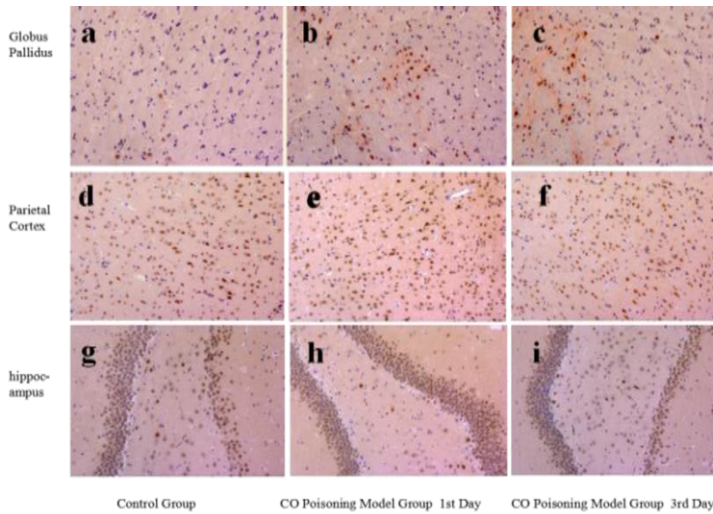


Figure 4. Immunohistochemical analysis of the heme oxygenase-1, (a)(d)(g) The normal control rats ($HO-1 \times 200$), (b)(e)(h) The CO exposure group in first day ($HO-1 \times 200$), (c)(f)(i) The CO exposure group in third day ($HO-1 \times 200$).

4. Discussion

A study of autopsy findings of damaged brain from CO poisoning by Lapresle and Fardeau [16], which identified 1) necrosis in the GP, 2) demyelination in the CWM, 3) spondylotic changes in the cerebral cortex, and 4) necrosis in the hippocampus. However, whether the pathological demyelination and metabolic changes are seen in the early stage after CO poisoning remains unknown.

DKI scanning can simultaneously measure multiple parameters, such as FA, MD, MK, which could reflect most of the microstructure changes in the brain [10, 11, 17]. The results of Cheung, et al. [17] demonstrated that, DKI offers a more comprehensive and sensitive detection of tissue microstructural changes, it can provide a better MR diffusion characterization of neural tissues, both WM and GM, in normal, developmental and pathological states [17]. Therefore, we hypothesize that DKI can be beneficial in improving the early depiction of delayed encephalopathy in patients after acute CO intoxication, we analyze MK, FA and MD in both WM and GM regions in our study.

Reduced ADC has been observed both in the acute and delayed relapse phases in patients with CO intoxication and indicates cytotoxic edema, these reports documented that areas of signal hyperintensity and low ADC in the CWM remained in the subacute and chronic phases, as in the acute phase. From a pathologic perspective, these findings suggest progressive demyelination with cytotoxic edema. Previous DWI studies showed that CO poisoning presented differently from cerebral infarction (i.e., decreased ADC lasting 3-5 days, and recovered in 1-4 weeks after the onset). The damage to the white matter due to CO poisoning cannot simply be explained using ischemic changes [18]. Our study showed a significant decreased MD value occurred in the globus pallidus, hippocampus and parietal cortex both in day1 and day3 after CO poisoning, however, the changes of pathological manifestations were different among

them. MD value changes in early state cannot reflect the pathological progressive of CO-poisoning-related encephalopathy in WM or GM.

Our study showed only limited regions of FA decreases in the acute stage of CO exposure, lower FA values were found in the hippocampus and no significant differences in the parietal lobe and globus pallidus between the CO exposed and normal control rats. Decreases of FA value here may only reveal an increase of the extracellular volume and/or possibly altered fiber integrity due to demyelination and axonal loss.

MK, as an important parameter of DKI, In the present study, significant decreases of MK values in the hippocampus and parietal cortex and increases in the globus pallidus were observed after CO poisoning, which associated with difference pathological manifestations.

A decrease in MK values in the hippocampus and parietal cortex could be explained as former study [19], during acute carbon monoxide poisoning, inhaled CO enters the alveoli, then diffuses through aveolar membrane into the blood and conjugates with hemoglobin (Hb). The dissociation rate of COHb is 1/3600 of oxyhemoglobin (O₂Hb), therefore, COHb blocks the transport of oxygen, resulting in reduced blood oxygen levels. Hypoxia can cause brain cell edema, acidosis, and increased blood-brain barrier permeability. The resulting increased intracellular osmotic pressure promotes the intracellular transportation of water molecules and cell swelling, so causing cytotoxic edema. The autoimmune responses and free radicals induce lipid peroxidation, leading to demyelination of the nerve fibers and reducing the limiting water diffusion through myelin [19]. This reduced restriction of water molecule diffusion reduces MK values in this way. The pathological studies showed significant edema in the hippocampus and parietal cortex, although with reduced the number of nervous cells, lightly stained cytoplasm, but no significant apoptosis or inflammatory cell infiltration were found. The decreased MK values suggesting a reduction in diffusional heterogeneity, reflect the immediate pathological changes of cytotoxic edema.

However, pathological findings confirmed the condition in the globus pallidus, which with increased MK values in vivo, were more seriously than that in the hippocampus and parietal cortex region. The reasons for increased MK values in the globus pallidus include the fact that the globus pallidus is located in areas supplied by terminal branches of the middle cerebral artery with less collateral circulation. During acute CO poisoning, vascular endothelial cells undergo degeneration and necrosis due to hypoxia and acidosis. Then the rough intima causes platelet aggregation and thrombus formation. The changes cause diffused brain ischemia, hypoxia, myelination, followed by degeneration of the brain endothelial cells of the arterioles due to hypoxia. With disease progression, demyelination, axonal injuries, neuronal necrosis, and inflammatory infiltration caused by autoimmune responses caused significantly higher local tissue complexity in the globus pallidus and significantly limited diffusion of water molecules. In this way, the MK values were abnormally elevated. Pathological findings also confirmed that in the globus pallidus were consistent with the pathological progress of acute carbon monoxide intoxication [20]. No significant correlations between the MK values and the carboxyhemoglobin levels could be established in our study.

The increased expression of HO-1 may be involved in the pathogenesis of brain injury induced by carbon monoxide poisoning, which changes the expression of apoptosis-related proteins and promotes the apoptosis of nerve cells [21, 22]. The result

of immunohistochemical experiments of the heme oxygenase-1 of rats in present study showed the IOD of the heme oxygenase-1 expression in the globus pallidus were increased in the CO poisoning group, there were a statistical difference between the CO poisoning group and the normal group both in the day 1 and day 3. On the contrary, there are no statistically significant difference of the IOD of the heme oxygenase-1 expression in the the hippocampus and parietal cortex between the CO poisoning group and the normal group both in the day 1 or day 3. These findings were consistent with the DKI findings, MK values increased only in globus pallidus with a statistical difference between the CO poisoning group and the normal group both in the day 1 and day 3. These results indicated that the MK value could be a more sensitive biomarker for early detection microstructural changes and encephalopathy of CO intoxication than the conventional DTI-related indices.

The amount of COHb formed and the manifestation of toxic effects relate to the concentration and the duration of CO exposure. While, exposure to CO concentrations in excess of 200 ppm results in COHb levels of approximately 30% and readily causes headache, dizziness, and impaired judgment, and inspiring >800 ppm CO is considered a high concentration exposure and results in COHb levels that exceed 60% and can rapidly lead to seizures, coma, and death in human [23]. However, no significant correlation between the carboxyhemoglobin levels and the different neuropsychological symptoms of the patients was found in a retrospective study. In our study, the blood HbCO levels of rats were an average of 64.53%, DKI-related indices, no significant correlations with COHb levels were found. Our results further prove that DKI may more beneficial in the assessment of acute brain injury following CO poisoning than the COHb levels in the blood.

To the best of our knowledge, our study is the first DKI investigation to assess the WM and GM abnormalities of the acute CO rats. DKI is superior to DTI in detecting early CO-induced white matter and gray matter injury, it can reflect the pathological progressive of CO-poisoning-related encephalopathy in WM or GM.

There are several limitations in this study. First, we only chose the globus pallidus, hippocampus, and parietal cortex as ROIs. It would be of great interest to examine other regional brain changes. Second, we didn't analyse all DKI-related indices, such as AK and RK data. It would be advantageous to analyze all DKI values to figure out more detail of brain microstructure changes. Finally, the duration time for the DKI scan was too long. Therefore, future studies will attempt to optimize the scanning parameters.

5. Conclusion

DKI can possess sufficient sensitivity for tracking pathophysiological changes associated with carbon monoxide intoxication. In acute carbon monoxide poisoning, the higher MK values indicated poor prognosis in the evolution of the condition. Vulnerability of the globus pallidus, hippocampus and parietal cortex to effects of acute carbon monoxide intoxication suggests that changes in DKI of the brain in vivo may be useful in predicting clinical outcome and facilitating early interventions that might reduce more serious sequelae following acute carbon monoxide intoxication.

Acknowledgments

This study was funded by the Joint Research Fund for Enterprise and basic and applied basic research Programs of Guangdong Province of China (Grant No. 2021A1515 220112), and Special Funds of Department of Science and Technology of Guangdong Province (Grant Number: 202055, 202063) and was supported by the Project of Traditional Chinese Medicine Bureau of Guangdong Province (Grant Number: 20202093). WZ has received these research grants.

References

- [1] Wang L, Wang A, Supplee W W, Koffler K, Cheng Y, Quezado Z M N, et al. Data on the effect of sex on the size, cellular content, and neuronal density of the developing brain in mice exposed to isoflurane and carbon monoxide. *Data Brief*. 2017;13:550-56.
- [2] Cheng Y, Thomas A, Mardini F, Bianchi S L, Tang J X, Peng J, et al. Neurodevelopmental consequences of sub-clinical carbon monoxide exposure in newborn mice. *PLoS One*. 2012;7(2):e32029.
- [3] Sharma P, Eesa M, Scott J N. Toxic and acquired metabolic encephalopathies: MRI appearance. *AJR Am J Roentgenol*. 2009;193(3):879-86.
- [4] Durak A C, Coskun A, Yikilmaz A, Erdogan F, Mavili E, Guven M. Magnetic resonance imaging findings in chronic carbon monoxide intoxication. *Acta Radiol*. 2005;46(3):322-27.
- [5] Mukherjee P, McKinstry R C. Diffusion tensor imaging and tractography of human brain development. *Neuroimaging Clin N Am*. 2006;16(1):19-43, vii.
- [6] Kim J H, Chang K H, Song I C, Kim K H, Kwon B J, Kim H C, et al. Delayed encephalopathy of acute carbon monoxide intoxication: diffusivity of cerebral white matter lesions. *AJNR Am J Neuroradiol*. 2003;24(8):1592-97.
- [7] Lin W C, Lu C H, Lee Y C, Wang H C, Lui C C, Cheng Y F, et al. White matter damage in carbon monoxide intoxication assessed in vivo using diffusion tensor MR imaging. *AJNR Am J Neuroradiol*. 2009;30(6):1248-55.
- [8] Beppu T. The role of MR imaging in assessment of brain damage from carbon monoxide poisoning: a review of the literature. *AJNR Am J Neuroradiol*. 2014;35(4):625-31.
- [9] Johnson V E, Stewart W, Smith D H. Axonal pathology in traumatic brain injury. *Exp Neurol*. 2013;24(6):35-43.
- [10] Jensen J H, Helpert J A. MRI quantification of non-Gaussian water diffusion by kurtosis analysis. *NMR Biomed*. 2010;23(7):698-710.
- [11] Zheng H, Lin J, Lin Q, Zheng W. Magnetic resonance image of neonatal acute bilirubin encephalopathy: A diffusion kurtosis imaging study. *Frontiers in Neurology*. 2021 August;12:645534.
- [12] Chou M C, Li J Y, Lai P H. Longitudinal white matter changes following carbon monoxide poisoning: A 9-month follow-up voxelwise diffusional kurtosis imaging study. *AJNR Am J Neuroradiol*. 2019;40(3):478-82.
- [13] Fountain S B, Raffaele K C, Annau Z. Behavioral consequences of intraperitoneal carbon monoxide administration in rats. *Toxicol Appl Pharmacol*. 1986;83(3):546-55.
- [14] Paxinos G, Watson C. *The Rat Brain in Stereotaxic Coordinates-the New Coronal Set*. 5th edition. Elsevier Academic Press, San Diego. 2005.
- [15] Hu C, Jensen J H, Falangola M F, Helpert J A. CSF partial volume effect for diffusional kurtosis imaging. *Proc. Int. Soc. Magn. Reson. Med. Toronto, Canada*. 2008;16,3325.
- [16] Lapresle J, Fardeau M. The central nervous system and carbon monoxide poisoning. II. Anatomical study of brain lesions following intoxication with carbon monoxide (22 cases). *Prog Brain Res*. 1967;24:31-74.
- [17] Cheung M M, Hui E S, Chan K C, Helpert J A, Qi L, Wu E X. Does diffusion kurtosis imaging lead to better neural tissue characterization? A rodent brain maturation study. *Neuroimage*. 2009;45(2):386-92.
- [18] Chu K, Jung K H, Kim H J, Jeong S W, Kang D W, Roh J K. Diffusion-weighted MRI and 99mTc-HMPAO SPECT in delayed relapsing type of carbon monoxide poisoning: Evidence of delayed cytotoxic edema. *Eur Neurol*. 2004;51(2):98-103.
- [19] Kinoshita T, Sugihara S, Matsusue E, Fujii S, Ametani M, Ogawa T. Pallidoreticular damage in acute carbon monoxide poisoning: diffusion-weighted MR imaging findings. *AJNR Am J Neuroradiol*. 2005;26(7):1845-48.

- [20] Okeda R, Funata N, Takano T, Miyazaki Y, Higashino F, Yokoyama K, et al. The pathogenesis of carbon monoxide encephalopathy in the acute phase--physiological and morphological correlation. *Acta Neuropathol.* 1981;54(1):1-10.
- [21] Maines M D. The heme oxygenase system and its functions in the brain. *CellMol Biol(Noisy-le-grand).* 2000;46(3):573-85.
- [22] Mecoubrey W K, mainnes M D. The structure organization and differential expression of the gene coding rat heme oxygenase. *Gene.* 1994;139:155-61.
- [23] Winter P M, Miller J N. Carbon monoxide poisoning. *Jama.* 1976;236(13):1502.